

Analytical Methods

Accepted Manuscript



This is an *Accepted Manuscript*, which has been through the Royal Society of Chemistry peer review process and has been accepted for publication.

Accepted Manuscripts are published online shortly after acceptance, before technical editing, formatting and proof reading. Using this free service, authors can make their results available to the community, in citable form, before we publish the edited article. We will replace this *Accepted Manuscript* with the edited and formatted *Advance Article* as soon as it is available.

You can find more information about *Accepted Manuscripts* in the [Information for Authors](#).

Please note that technical editing may introduce minor changes to the text and/or graphics, which may alter content. The journal's standard [Terms & Conditions](#) and the [Ethical guidelines](#) still apply. In no event shall the Royal Society of Chemistry be held responsible for any errors or omissions in this *Accepted Manuscript* or any consequences arising from the use of any information it contains.

1
2
3 1 **Preparation and characterization of graphene quantum dots-Fe₃O₄**
4
5
6 2 **nanocomposite as an efficient adsorbent in magnetic solid phase extraction:**
7
8 3 **Application to determination of Bisphenol A in water samples**
9
10
11
12 4

14 5 Rahim Mohammad-Rezaei, Habib Razmi*, Vahideh Abdollahi, Amir Abbas Matin

17
18 6 *Analytical Chemistry Research Lab., Faculty of Basic Sciences, Azarbaijan Shahid Madani*
19
20 7 *University, P.O. Box: 53714-161, Tabriz, Iran*
21

22 8
23
24 9 *Tel.: +984124327500*
25

26
27 10 *Fax: +984124327541*
28

29 11
30
31

32 12
33
34

35 13
36
37

38 14
39
40

41 15
42
43

44 16
45
46

47 17
48
49

50 18
51
52

53
54
55 _____
56 *Corresponding author

57 E-mail: h.razmi@azaruniv.edu
58
59
60

1 Abstract

2 This study describes the preparation, characterization and application of graphene quantum
3 dots coated Fe_3O_4 ($\text{Fe}_3\text{O}_4/\text{GQDs}$) magnetic nanocomposite as a novel adsorbent for magnetic
4 solid phase extraction (MSPE). The $\text{Fe}_3\text{O}_4/\text{GQDs}$ was synthesized by a simple hydrothermal
5 method and the resultant nanocomposite was characterized by X-ray powder diffraction, field
6 emission scanning electron microscopy and Fourier transform infrared. The prepared
7 nanocomposite was used for preconcentration and determination of Bisphenol A (BPA) in
8 drinking water samples using high performance liquid chromatography with ultraviolet
9 detection (HPLC-UV). Under the optimal extraction and analytical conditions, the developed
10 method demonstrated a wide dynamic linear range ($0.1\text{-}300\text{ ng mL}^{-1}$), good linearity
11 ($R^2=0.9958$), low detection limit (12.3 pg mL^{-1}) and high enrichment factor (360). The
12 developed MSPE-HPLC-UV method was successfully applied to determination of leaked
13 BPA from plastic bottle into the drinking water samples after exposing it to the sunlight.
14 Satisfactory recoveries showed that the matrices under consideration do not significantly
15 affect the extraction process. The adsorption efficiencies of $\text{Fe}_3\text{O}_4/\text{GQDs}$, $\text{Fe}_3\text{O}_4/\text{graphene}$
16 and unmodified magnetic Fe_3O_4 nanoparticles were comparatively studied in the
17 preconcentration and determination of BPA by HPLC-UV. Based on experimental results,
18 $\text{Fe}_3\text{O}_4/\text{GQDs}$ exhibit improved adsorption behaviour due to unique surface properties of
19 GQDs.

20
21 Keywords: graphene quantum dots; Bisphenol A; magnetic nanocomposite

1. Introduction

Bisphenol A (2,2-bis(4-hydroxyphenyl)propane, BPA), is a member of diphenols in which two phenolic rings are joined together through a isopropylidene bridging group. It is the main ingredient used for the production of polycarbonate, epoxy, polyester, and polysulfone resins¹. BPA is also used as a component of synthetic plastic materials² and antioxidants in glue sand inks^{3,4}. Recent studies indicate that BPA and its derivatives have high potential as endocrine disruptors in humans and wildlife^{5,6}. Thus the effect of BPA on human health through beverage, food, and water has generated great concern during the recent years.

The polarity and low concentrations of BPA in real samples cause significant problems in devising appropriate analytical methods. The literature on the analysis of BPA and its derivatives reveal that liquid-liquid extraction (LLE)⁷⁻⁹ and solid-phase extraction (SPE)^{10,11} have usually been used for isolation and preconcentration of these compounds. Due to the some disadvantages such as intensive labor, time consuming, unsatisfactory enrichment factor and large quantity of toxic solvent, the use of LLE is limited in separation science. In SPE based sample preparation methods, there is a solid-phase adsorbent which adsorbs the analyte from the sample matrix and results a pre-purified, concentrated and compatible analyte with the analytical system. In some cases, due to the limited rate of diffusion and mass transfer, extraction time of SPE processes is too long.

Recently increasing number of studies have been concentrated on adsorption and separation using magnetic materials¹²⁻¹⁴ which is so-called magnetic solid-phase extraction (MSPE). This technique is based on the combination of magnetic inorganic material and non-magnetic adsorbent material. By taking the advantage of both materials, the MSPE technology exhibits excellent adsorption efficiency and rapid separation from the matrix by an external magnetic field. On the other hand, rapid mass transfer can be obtained due to the sufficiently large contact area between the sorbents and the analytes, which is beneficial for

1
2
3 1 rapid equilibrium. Magnetic separation based on the super paramagnetic Fe_3O_4 is obviously
4
5 2 much more convenient, economic and efficient ¹⁵⁻¹⁷. The most important component of the
6
7 3 MSPE is the adsorbent material, which dominates the selectivity and sensitivity of the
8
9 4 method.

10
11 Graphene, a new class of 2D carbon nanomaterial with one-atom thickness, has
12
13 6 attracted considerable attention in recent years. Due to the presence of oxygen containing
14
15 7 groups such as hydroxyl, epoxy, carbonyl, and carboxyl groups, graphene and graphene oxide
16
17 8 have been frequently used in separation science ¹⁸⁻²⁰. Graphene quantum dots (GQDs), are
18
19 9 graphene sheets that are smaller than 100 nm and has been emerged as a significant research
20
21 10 area in recent years ²¹⁻²⁴. GQDs having various electronic and optoelectronic properties due to
22
23 11 quantum confinement and edge effects, making it an excellent candidate for construction of
24
25 12 nanoscaled optical and electronic devices. GQDs are superior to common carbon materials
26
27 13 because the nature of nano-sized single layer graphene sheets which endows them ultrahigh
28
29 14 specific surface and makes GQDs more sensitive to the environmental changes.

30
31
32 In the present study, $\text{Fe}_3\text{O}_4/\text{GQDs}$ nanocomposite was synthesized successfully and
33
34 15 characterized by X-ray diffraction (XRD), Fourier transform infrared spectroscopy (FTIR),
35
36 16 and field emission scanning electron microscopy (FESEM). The prepared $\text{Fe}_3\text{O}_4/\text{GQDs}$ was
37
38 17 employed for preconcentration of BPA from aquatic samples using MSPE method prior to
39
40 18 determination by HPLC-UV. To evaluate the applicability of the proposed method, it was
41
42 19 applied to the determination of released BPA from water containing bottles into the drinking
43
44 20 water samples.
45
46 21
47
48
49
50
51

52 23 **2. Experimental**

53 24 **2.1. Chemicals and water samples**

1
2
3 1 BPA was provided by Sigma-Aldrich (St. Louis, MO, USA). Standard solutions of BPA at a
4
5 2 concentration of 1000 mg L⁻¹ was prepared in methanol and stored at 4 °C. Methanol LC-
6
7 3 grade from Merck (Darmstadt, Germany) was used for the chromatographic analysis.
8
9 4 FeCl₂.4H₂O, FeCl₃.6H₂O, sodium hydroxide and hydrochloric acid were used to synthesis
10
11 5 magnetic nanoparticles (MNPs) and to adjust the solution pH. Also sodium chloride used for
12
13 6 ionic strength studies were purchased from Merck. All other chemicals were obtained from
14
15 7 Merck.

18
19 8 The recovery studies were carried out using mineral water samples that was collected
20
21 9 from kandowan mineral water (East Azarbaijan Province, Iran). For the study of leaked BPA
22
23 10 values from plastic bottles into the drinking water samples, the samples were stored in
24
25 11 polyethylene bottles. Before exposing water containing bottles in front of sunlight, they were
26
27 12 stored in refrigerator at 4 °C. The standard BPA solutions were prepared daily by diluting the
28
29 13 stock standard solutions to the required concentrations with ultra-pure water.
30
31
32 14

33 34 15 **2.2. Synthesis of graphene quantum dots (GQDs)**

35
36 16 In this study, the hydrothermal method was used for the synthesis of GQDs. Firstly, graphene
37
38 17 oxide was prepared by chemical oxidization of graphite powder according to the modified
39
40 18 Hummers method^{25,26}. The as prepared graphene oxide was deoxidized in a tube furnace at
41
42 19 250 °C for 2 hours at a heating rate of 5 °C min⁻¹ in a nitrogen atmosphere. The obtained
43
44 20 graphene sheets oxidized in concentrated H₂SO₄ (10 mL) and HNO₃ (30 mL) for 15 hours
45
46 21 under mild ultrasonication (500 W, 40 kHz). The oxidized graphene sheets were diluted and
47
48 22 purified with microporous membrane (retained 40 micrometre) and redispersed in deionized
49
50 23 water. Then the suspension was heated at 200 °C for 10 hours in an autoclave. The resulting
51
52 24 black suspension was filtered with microporous membrane and a brown filtered solution was
53
54 25 obtained. To remove larger graphene nanoparticles, the colloidal solution was dialyzed in a
55
56
57
58
59
60

1
2
3 1 dialysis bag (retained molecular weight: 3500 Da) overnight and GQDs were obtained having
4
5 2 stability more than 3 months.
6
7 3

4 **2.3. Synthesis of Fe₃O₄ nanoparticles**

5 Fe₃O₄ nanoparticles were prepared according to the modified Massart method ²⁷ via the co-
6 precipitation of a mixture of FeCl₃.6H₂O and FeCl₂.4H₂O. In particular, FeCl₃.6H₂O (3.03 g)
7 and FeCl₂.4H₂O (1.13 g) were completely dissolved in 150 mL deionized water. The aqueous
8 solution was heated to 60 °C under vigorous agitation so as to obtain a clear yellow solution.
9 Then, aqueous ammonia solution was added dropwise until the pH of the solution reached the
10 value of 10. The reaction was maintained for an additional 30 min under vigorous stirring. N₂
11 was used as the protective gas throughout the experiment. After completing the reaction, the
12 black precipitate was collected by an external magnetic field, followed by washing several
13 times with deionized water and ethanol.
14

15 **2.4. Synthesis of Fe₃O₄/GQDs nanocomposite**

16 Firstly, GQDs (0.1 g) was dispersed in 150 mL deionized water by sonication for 10 min.
17 Then, 1.214 g FeCl₃.6H₂O was added to the GQDs solution at room temperature under a
18 nitrogen flow with vigorous stirring. Then temperature was raised to 80 °C and 0.485 g of the
19 FeCl₂.4H₂O were added slowly to the solution containing Fe₃⁺-GQDs which was vigorously
20 stirred for additional 30 min. Finally, the ammonia solution was added dropwise to adjust the
21 pH of the solution at 10 for synthesis of magnetite Fe₃O₄/GQDs. Fe₃O₄/graphene was
22 synthesized with same procedure, and just graphene was added instead of GQDs in the
23 synthesis process.
24

25 **2.5. Instrumentation**

1
2
3 1 A Jasco HPLC system, consisted of a PU-1580 isocratic pump, a Rheodyne 7725i injector
4
5 2 with a 10- μ L loop (Rheodyne, Cotati, CA, USA) and a UV-1575 spectrophotometric detector
6
7 3 were used in the experiment. The chromatographic system was controlled by HSS-2000
8
9 4 provided by Jasco using the LC-Net II/ADC interface. The data were processed using
10
11 5 BORWIN software (version 1.50). An analytical 250 \times 4.6 mm ID, 5 μ m particle, Perfectsil
12
13 6 Target ODS-3 column (MZ-Analysen technik, Germany) with a ODS-3 pre-column (10 \times 4.0
14
15 7 mm I.D., 5 μ m), which was maintained at ambient temperature, was employed for separation.
16
17 8 X-ray diffraction (XRD) was performed by using a Bruker AXD (D8 Advance) X-ray
18
19 9 powder diffractometer with a Cu K α radiation source ($\lambda=0.154056$ nm) generated at 40 kV
20
21 10 and 35 mA. Fourier transform infrared (FT-IR) spectra were recorded using a Bruker model
22
23 11 Vector 22 FT IR Spectrometer (Ettlingen, Germany) on KBr pellets. Field emission scanning
24
25 12 electron microscopy (FESEM) images were obtained using an S-4800 field emission
26
27 13 scanning electron microscope (Hitachi, Tokyo, Japan).
28
29
30
31
32
33

34 15 **2.6. MSPE Procedure**

35
36 16 MSPE of all the samples involved in this study was carried out as follows: 600 mL aliquot
37
38 17 filtered water samples at a concentration of 100 ng mL⁻¹ was transferred to 1000 mL
39
40 18 glassware beakers. Then 50 mg of Fe₃O₄/GQDs nanocomposite was added into the sample
41
42 19 solution and was stirred for 20 min at 25 °C. Afterward an Nd-Fe-B magnet (100 \times 50 \times 40 mm)
43
44 20 was positioned at the bottom of the breaker and Fe₃O₄/GQDs nanocomposite was isolated
45
46 21 from the solution. The preconcentrated BPA adsorbed on Fe₃O₄/GQDs nanocomposite was
47
48 22 desorbed with 1 mL methanol at 25 °C. A 10 μ L of the concentrated solution was injected
49
50 23 into the HPLC system for analysis.
51
52
53
54
55

56 25 **2.7. Chromatographic conditions**

1
2
3 1 The isocratic mobile phase consisted of methanol-water in the ratio of 70:30 v/v, flowing
4
5 2 through the column at a constant flow rate of 1 mL min⁻¹. The eluent was monitored using
6
7 3 UV detection at a wave length of 278 nm. The mobile phase was filtered through a 0.22 μm
8
9 4 membrane-type GV filter (Millipore). A 40 kHz and 138W ultrasonic water bath with
10
11 5 temperature control (sonic bath model LBS2-FALC instruments SRL Treviglio, Italy) was
12
13 6 applied to degassing the mobile phase.
14
15
16
17
18

19 8 **3. Results and discussion**

20 9 **3.1. Characterization of Fe₃O₄ and Fe₃O₄/GQDs**

21
22
23 10 The surface chemistry of Fe₃O₄ and Fe₃O₄/GQDs was studied using FTIR. The typical FTIR
24
25 11 spectra of magnetic nanoparticles were shown in Fig. 1. As can be seen the Fe-O band at
26
27 12 Fe₃O₄/GQDs (611 cm⁻¹) shifted to higher wavelength in comparison with Fe₃O₄ (580 cm⁻¹)
28
29 13 indicating the bonding of Fe₃O₄ to C-O-H groups on GQDs surface ²⁸. An absorption band
30
31 14 appeared at 3411 cm⁻¹ corresponding to hydroxyl groups on Fe₃O₄ and Fe₃O₄/GQDs surface
32
33 15 and the peak at 1618 cm⁻¹ corresponding to vibration of water molecules adsorbed on Fe₃O₄
34
35 16 and Fe₃O₄/GQDs surfaces. Strong bond at 1605 cm⁻¹ corresponding to stretching frequencies
36
37 17 of C=C on Fe₃O₄/GQDs surface. Peaks at 908 cm⁻¹ and 1065 cm⁻¹ can be correspond to
38
39 18 stretching frequencies of C-C at Fe₃O₄/GQDs and the peaks at 1258 cm⁻¹ and 1384 cm⁻¹
40
41 19 corresponding to the C-O stretching and O-H bending vibrations ²⁹⁻³¹. The presence of
42
43 20 hydrophilic GQDs composited to the Fe₃O₄ provided an appropriate media for strong surface
44
45 21 adsorption of BPA on the sorbent.
46
47
48

49
50 22 The crystalline structure of the synthesized MNPs was characterized by XRD. The
51
52 23 XRD spectra of the Fe₃O₄ and the Fe₃O₄/GQDs were shown in Fig. 2. The presence of the
53
54 24 peaks corresponding to the (220), (311), (400), (422), (511), and (440) planes at the 2θ of 30,
55
56 25 36, 44, 54, 57 and 63 degrees confirm the formation of spinel structure ³². Also, Fe₃O₄ and
57
58
59
60

1
2
3 1 Fe₃O₄/GQDs MNPs has similar diffraction peaks, which indicate that the crystal structure of
4
5 2 Fe₃O₄ was not changed after modification with GQDs.

6
7 3 Fig. 3 shows the FESEM images of Fe₃O₄ (left) and Fe₃O₄/GQDs (right), obtained with
8
9
10 4 60000 magnifications. It can be seen that the Fe₃O₄ have nearly uniform distribution of
11
12 5 particle size. The particle sizes of both Fe₃O₄ and Fe₃O₄/GQDs were measured in FESEM
13
14 6 micrographs. The diameter of Fe₃O₄ is 42 nm and that of Fe₃O₄/GQDs is a little larger.
15
16
17 7

18 8 **3.2. Optimization of extraction process**

19 9 **3.2.1. Effect of pH**

20
21
22
23 10 The solution pH will change the surface charge of Fe₃O₄/GQDs, which is a primary factor
24
25 11 affecting the adsorption towards the analyte. Here, the influence of the sample pH on the
26
27 12 extraction efficiency was investigated by adjusting the pH in the range 3-12. The effect of pH
28
29 13 value on the recoveries of BPA is shown in Fig. 4. It can be seen that the recoveries increased
30
31 14 as the pH was increased from 3 to 5.2, and above pH 5.2, the recovery decreased. Surface
32
33 15 charge and also the stability of the Fe₃O₄/GQDs should be considered in pH study. In more
34
35 16 acidic media, iron oxide gets dissolved and the recoveries decreases. Also at more acidic
36
37 17 media, due to electrostatic repulsion between Fe₃O₄ and GQDs, the stability of Fe₃O₄/GQDs
38
39 18 decrease and the recoveries are low³³. At high basic media, BPA exists in deprotonated form
40
41 19 (the pK_a value of BPA in aqueous solutions is 9.8) and thus the interaction between
42
43 20 Fe₃O₄/GQDs surface and BPA is very weak. At pH 5.2, the stability of Fe₃O₄/GQDs
44
45 21 nanocomposite is high and tendency between the charge of GQDs functional groups and BPA
46
47 22 is well. Therefore, pH 5.2 was selected as working pH.
48
49
50
51
52 23

53 24 **3.2.2. Effect of nano-sorbent amount**

1
2
3 1 The effect of Fe₃O₄/GQDs dosage on the extraction efficiency of BPA from aqueous samples
4
5 2 is presented in Fig. 5. The peak areas increased with increasing the sorbent amount from 5 to
6
7 3 50 mg, and stayed unchanged with further increases. This result indicated that 50 mg of nano-
8
9 4 sorbent was sufficient to extract BPA from aqueous solution. Therefore in the following
10
11 5 experiments 50 mg of Fe₃O₄/GQDs was used to ensure the complete adsorption of BPA.
12
13

14 **3.2.3. Effect of ionic strength**

15
16 7 Generally addition of salt decreases the solubility of analytes in aqueous samples and
17
18 8 enhances their partitioning into the adsorbent or organic phases. The effect of ionic strength
19
20 9 on the extraction efficiency was studied by addition of sodium chloride at 0-20 % (w/v). In
21
22 10 this study the extraction efficiency of the prepared sorbent was increased poorly with
23
24 11 increasing sodium chloride, but precision of the process decreased with increasing the salt.
25
26 12 Therefore, no salt was added in the followed experiments.
27
28
29
30
31

32 **3.2.4. Effect of desorption solvent**

33
34 15 After adsorption, BPA should be desorbed using an organic solvent from Fe₃O₄/GQDs for
35
36 16 HPLC analysis. To choose an optimum desorption solvent, five solvent were evaluated
37
38 17 (Methanol, Ethanol, Acetonitrile, Acetone and n-hexane) which are HPLC compatible
39
40 18 solvents. The results showed that Methanol has higher extraction efficiency in comparison
41
42 19 with other solvents (Fig. 6). Therefore, Methanol was chosen as desorption solvent.
43
44
45
46
47

48 **3.2.5. Effect of desorption time**

49
50 22 Desorption time is also a very important parameter due to its effect on desorption quantity
51
52 23 and sensitivity. BPA adsorbed by the sorbent, were desorbed with shaking the sorbent in
53
54 24 methanol for appropriate amount of time. The effect was studied by recording the peak area
55
56
57
58
59
60

1
2
3 1 versus desorption time. Fig. 7 shows desorption time profile from 5 to 50 min, where a 20
4
5 2 min desorption time appeared to be the optimum value for analysis.
6
7 3
8

9 10 4 **3.2.6. Break through volume**

11 5 Break through volume (the maximum volume that can be pre-concentrated with quantitative
12 6 recovery of analyte) is a major parameter in SPE and preconcentration of samples. It
13 7 significantly affects the preconcentration factor, the reproducibility and reliability of results.
14 8 The break through volume was determined by a series of different volume aqueous solutions
15 9 (50 to 600 mL) spiked with fixed amount of BPA at optimized conditions. Recovery of BPA
16 10 was found to be quantitative when sample volume was chosen between the ranges 50-600
17 11 mL. Above 600 mL, the time required to collect the suspension with magnet increases. So, by
18 12 analysing 1 mL of the final solution after the preconcentration of 600 mL sample solution, the
19 13 enrichment factor (EF) was found as 360.
20
21
22
23
24
25
26
27
28
29
30
31
32
33

34 15 **3.3. Validation of the method**

35 16 Quantitative parameters of the proposed method such as linear range (LR), coefficient of
36 17 determination (R^2), limit of detection (LOD), limit of quantification (LOQ), enrichment
37 18 factor (EF) and precision were evaluated under optimum conditions (Table 1). The
38 19 calibration curve were established using 600 mL deionized water spiked with different
39 20 concentrations of BPA. To obtain the precision of the method, replicated analysis of spiked
40 21 water samples were carried out for three times, and relative standard deviation (R.S.D.)
41 22 values were calculated by the obtained peak area. The LOD, based on signal-to-noise ratio
42 23 (S/N) of 3, was 12.3 pg mL^{-1} and the LOQ, based on S/N of 10, was 41 pg mL^{-1} .
43
44
45
46
47
48
49
50
51
52
53
54
55

56 25 **3.4. Comparison**

57
58
59
60

1
2
3 1 Extraction efficiency of BPA from aqueous solution with SPME method by using Fe_3O_4 ,
4
5 2 Fe_3O_4 /graphene and Fe_3O_4 /GQDs sorbents that prepared at the same conditions are shown in
6
7 3 fig. 8. As can be seen, Fe_3O_4 shows no efficiency in the extraction of BPA. The presence of
8
9 4 graphene sheets in Fe_3O_4 /graphene increased the extraction efficiency. The result of this
10
11 5 observation can be related to the π - π interactions between graphene sheets and aromatic rings
12
13 6 of BPA. When enormous graphene sheets in Fe_3O_4 /graphene convert to very small GQDs
14
15 7 sheets in Fe_3O_4 /GQDs, the potential of sorbent in extraction of BPA increases outstandingly
16
17 8 which can be related to the high surface to volume ratio, high capacity of sorbent, present of
18
19 9 small sheets that have π - π interactions, and the present of hydroxyl functional groups that
20
21 10 results high polarity of GQDs.
22
23
24
25
26
27

28 12 **3.5. Analysis of real samples**

29
30 13 To test the reliability of the proposed procedure, the method was employed to determine the
31
32 14 trace amount of BPA in mineral water samples which were stored in polyethylene bottles and
33
34 15 investigation of leakage of BPA from polyethylene bottles to mineral water after remaining in
35
36 16 front of sunlight. The first analysis demonstrated 0.21 ng mL^{-1} BPA in fresh mineral water
37
38 17 sample (Fig. 9A). After one week that waters were kept in front of sunlight, the amount of
39
40 18 BPA in water samples were increased to 3.4 ng mL^{-1} that shows the leakage of BPA from
41
42 19 polyethylene bottles to water samples (Fig. 9B). Fig. 9C shows the chromatogram of water
43
44 20 sample in polyethylene bottle after exposing to sunlight for one week and spiked with 20 ng
45
46 21 mL^{-1} BPA.

47
48
49 22 The accuracy of the method was evaluated by the recovery test which was carried out
50
51 23 with spiked mineral water samples. The recoveries for the analysis of BPA in spiked water
52
53 24 samples using the proposed method was shown in Table 2. According to these studies the
54
55
56
57
58
59
60

1
2
3 1 recoveries for BPA were in the range 96.3% to 104.9% with R.S.D. values between 3.6% and
4
5 2 5.2%.
6
7
8 3

9 4 **4. Conclusions**

10 5 In this study $\text{Fe}_3\text{O}_4/\text{GQDs}$ magnetic nano-sorbent was synthesized as a novel adsorbent for
11 6 magnetic solid phase extraction and applied for efficient enrichment of trace BPA from water
12 7 samples. The efficiency of $\text{Fe}_3\text{O}_4/\text{GQDs}$ in BPA preconcentration was compared with
13 8 $\text{Fe}_3\text{O}_4/\text{graphene}$ which resulted the improved adsorption behaviour of GQDs in comparison
14 9 with graphene. The results showed that the proposed method is suitable for rapid
15 10 preconcentration and determination of BPA from large volume samples. The method was
16 11 successfully applied to determination of leaked BPA from plastic bottle into the drinking
17 12 water samples. The high breakthrough volume of water samples and the small volume of the
18 13 elution permitted to get high enrichment factor. Due to the high capacity and surface to
19 14 volume ratio of GQDs in comparison with another carbon based materials, it can be used as
20 15 an efficient sorbent in separation science.
21
22
23
24
25
26
27
28
29
30
31
32
33
34
35
36
37
38
39
40
41
42
43
44
45
46
47
48
49
50
51
52
53
54
55
56
57
58
59
60

17 **Acknowledgement**

18 The authors gratefully acknowledge the Research Council of Azarbaijan Shahid Madani
19 University for financial support.
20
21
22
23
24
25

1
2
3 **1 Figure captions**
4

5 2 Fig. 1. FTIR spectra of the Fe_3O_4 and $\text{Fe}_3\text{O}_4/\text{GQDs}$ MNPs.
6

7 3 Fig. 2. XRD patterns of Fe_3O_4 and $\text{Fe}_3\text{O}_4/\text{GQDs}$ MNPs.
8

9 4 Fig. 3. FESEM images of Fe_3O_4 and $\text{Fe}_3\text{O}_4/\text{GQDs}$ MNPs.
10

11 5 Fig. 4. The effect of pH on the extraction efficiency.
12

13 6 Fig. 5. The effect of $\text{Fe}_3\text{O}_4/\text{GQDs}$ dosage on extraction efficiency of BPA.
14

15 7 Fig. 6. The effect of desorption solvent on extraction efficiency.
16

17 8 Fig. 7. The effect of desorption time on extraction efficiency.
18

19 9 Fig. 8. Comparison of extraction efficiency of BPA with Fe_3O_4 , $\text{Fe}_3\text{O}_4/\text{graphene}$ and
20 $\text{Fe}_3\text{O}_4/\text{GQDs}$ sorbents.
21

22 10 Fig. 9. The chromatograms of (A) fresh mineral water; (B) mineral water contained in plastic
23 bottle and exposed directly to sunlight for one week; (C) mineral water contained in
24 plastic bottle and exposed directly to sunlight for one week and spiked with 20 ng mL^{-1}
25 BPA.
26
27
28
29
30
31
32
33
34
35

36 11 Table. 1. Precision, LOQ, LOD, EF, linearity, and regression equation obtained in the
37 analysis of BPA.
38
39

40 12 Table 2. Results of determination and recoveries of mineral water samples spiked with BPA.
41
42
43
44
45
46
47
48
49
50
51
52
53
54
55
56
57
58
59
60

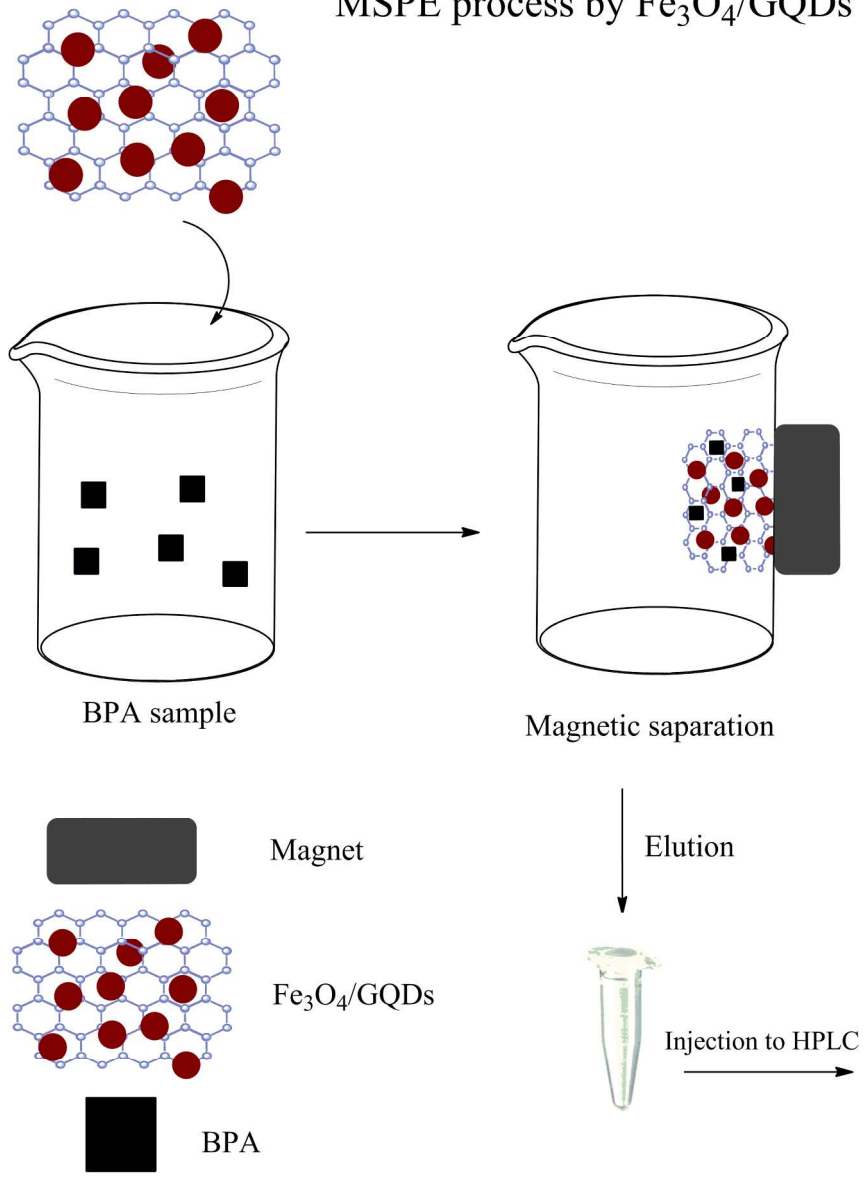
1
2
3 1 References
4

-
- 5 2 1. T. Geens, D. Aerts, C. Berthot, J.-P. Bourguignon, L. Goeyens, P. Lecomte, G. Maghuin-
6 3 Rogister, A.-M. Pironnet, L. Pussemier, M.-L. Scippo, J. Van Loco and A. Covaci, *Food and*
7 4 *Chemical Toxicology*, 2012, 50, 3725-3740.
 - 8 5 2. K. J. Wooten and P. N. Smith, *Chemosphere*, 2013, 93, 2245-2253.
 - 9 6 3. D. Pérez-Palacios, M. Á. Fernández-Recio, C. Moreta and M. T. Tena, *Talanta*, 2012, 99, 167-
10 7 174.
 - 11 8 4. K. Tarvainen, L. Kanerva, R. Jolanki and T. Estlander, *American Journal of Contact Dermatitis*,
12 9 1995, 6, 95-104.
 - 13 10 5. B. S. Rubin, *The Journal of Steroid Biochemistry and Molecular Biology*, 2011, 127, 27-34.
 - 14 11 6. P. Fenichel, N. Chevalier and F. Brucker-Davis, *Annales d'Endocrinologie*, 2013, 74, 211-220.
 - 15 12 7. N. Dorival-García, A. Zafra-Gómez, A. Navalón and J. L. Vilchez, *Talanta*, 2012, 101, 1-10.
 - 16 13 8. S. Errico, M. Bianco, L. Mita, M. Migliaccio, S. Rossi, C. Nicolucci, C. Menale, M. Portaccio, P.
17 14 Gallo, D. G. Mita and N. Diano, *Food Chemistry*, 2014, 160, 157-164.
 - 18 15 9. S. Liu, Q. Xie, J. Chen, J. Sun, H. He and X. Zhang, *Journal of Chromatography A*, 2013, 1295,
19 16 16-23.
 - 20 17 10. Z. Lin, W. Cheng, Y. Li, Z. Liu, X. Chen and C. Huang, *Analytica Chimica Acta*, 2012, 720, 71-76.
 - 21 18 11. F. Tan, H. Zhao, X. Li, X. Quan, J. Chen, X. Xiang and X. Zhang, *Journal of Chromatography A*,
22 19 2009, 1216, 5647-5654.
 - 23 20 12. K. Aguilar-Arteaga, J. A. Rodriguez and E. Barrado, *Analytica Chimica Acta*, 2010, 674, 157-
24 21 165.
 - 25 22 13. G. Giakissikli and A. N. Anthemidis, *Analytica Chimica Acta*, 2013, 789, 1-16.
 - 26 23 14. R. D. Ambashta and M. Sillanpää, *Journal of Hazardous Materials*, 2010, 180, 38-49.
 - 27 24 15. G. Dudek, R. Turczyn, A. Strzelewicz, M. Krasowska, A. Rybak and Z. J. Grzywna, *Separation*
28 25 *and Purification Technology*, 2013, 109, 55-63.
 - 29 26 16. L. Yang, Z. Gao, Y. Guo, W. Zhan, Y. Guo, Y. Wang and G. Lu, *Enzyme and Microbial*
30 27 *Technology*, 2014, 60, 32-39.
 - 31 28 17. B. Zhang, H. Zhang, X. Li, X. Lei, C. Li, D. Yin, X. Fan and Q. Zhang, *Materials Science and*
32 29 *Engineering: C*, 2013, 33, 4401-4408.
 - 33 30 18. S. Wang, H. Sun, H. M. Ang and M. O. Tadé, *Chemical Engineering Journal*, 2013, 226, 336-
34 31 347.
 - 35 32 19. L. Wang, X.-H. Zang, C. Wang and Z. Wang, *Chinese Journal of Analytical Chemistry*, 2014, 42,
36 33 136-144.
 - 37 34 20. K. Scida, P. W. Stege, G. Haby, G. A. Messina and C. D. García, *Analytica Chimica Acta*, 2011,
38 35 691, 6-17.
 - 39 36 21. H. Razmi and R. Mohammad-Rezaei, *Biosensors and Bioelectronics*, 2013, 41, 498-504.
 - 40 37 22. L. Li, G. Wu, G. Yang, J. Peng, J. Zhao and J.-J. Zhu, *Nanoscale*, 2013, 5, 4015-4039.
 - 41 38 23. Z.-b. Qu, X. Zhou, L. Gu, R. Lan, D. Sun, D. Yu and G. Shi, *Chemical Communications*, 2013, 49,
42 39 9830-9832.
 - 43 40 24. B. Wang, S. Zhuo, L. Chen and Y. Zhang, *Spectrochimica Acta Part A: Molecular and*
44 41 *Biomolecular Spectroscopy*, 2014, 131, 384-387.
 - 45 42 25. D. Pan, J. Zhang, Z. Li and M. Wu, *Advanced Materials*, 2010, 22, 734-738.
 - 46 43 26. S. Zuo, Y. Teng, H. Yuan and M. Lan, *Sensors and Actuators B: Chemical*, 2008, 133, 555-560.
 - 47 44 27. J. Li, X. Qiu, Y. Lin, X. Liu, R. Gao and A. Wang, *Applied Surface Science*, 2010, 256, 6977-6981.
 - 48 45 28. X. Lv, X. Xue, G. Jiang, D. Wu, T. Sheng, H. Zhou and X. Xu, *Journal of Colloid and Interface*
49 46 *Science*, 2014, 417, 51-59.
 - 50 47 29. G. He, W. Liu, X. Sun, Q. Chen, X. Wang and H. Chen, *Materials Research Bulletin*, 2013, 48,
51 48 1885-1890.
 - 52 49 30. Y.-P. Chang, C.-L. Ren, J.-C. Qu and X.-G. Chen, *Applied Surface Science*, 2012, 261, 504-509.

- 1 31. K. Singh, A. Ohlan, V. H. Pham, B. R. S. Varshney, J. Jang, S. H. Hur, W. M. Choi, M. Kumar, S.
- 2 K. Dhawan, B.-S. Kong and J. S. Chung, *Nanoscale*, 2013, 5, 2411-2420.
- 3 32. K. Zhang, Y. Zhang and S. Wang, *Sci. Rep.*, 2013, 3.
- 4 33. X. Liu, H. Zhu and X. Yang, *Talanta*, 2011, 87, 243-248.

1
2
3
4
5
6
7
8
9
10
11
12
13
14
15
16
17
18
19
20
21
22
23
24
25
26
27
28
29
30
31
32
33
34
35
36
37
38
39
40
41
42
43
44
45
46
47
48
49
50
51
52
53
54
55
56
57
58
59
60

MSPE process by $\text{Fe}_3\text{O}_4/\text{GQDs}$



MSPE process by $\text{Fe}_3\text{O}_4/\text{GQDs}$
178x248mm (300 x 300 DPI)

Analytical Methods Accepted Manuscript

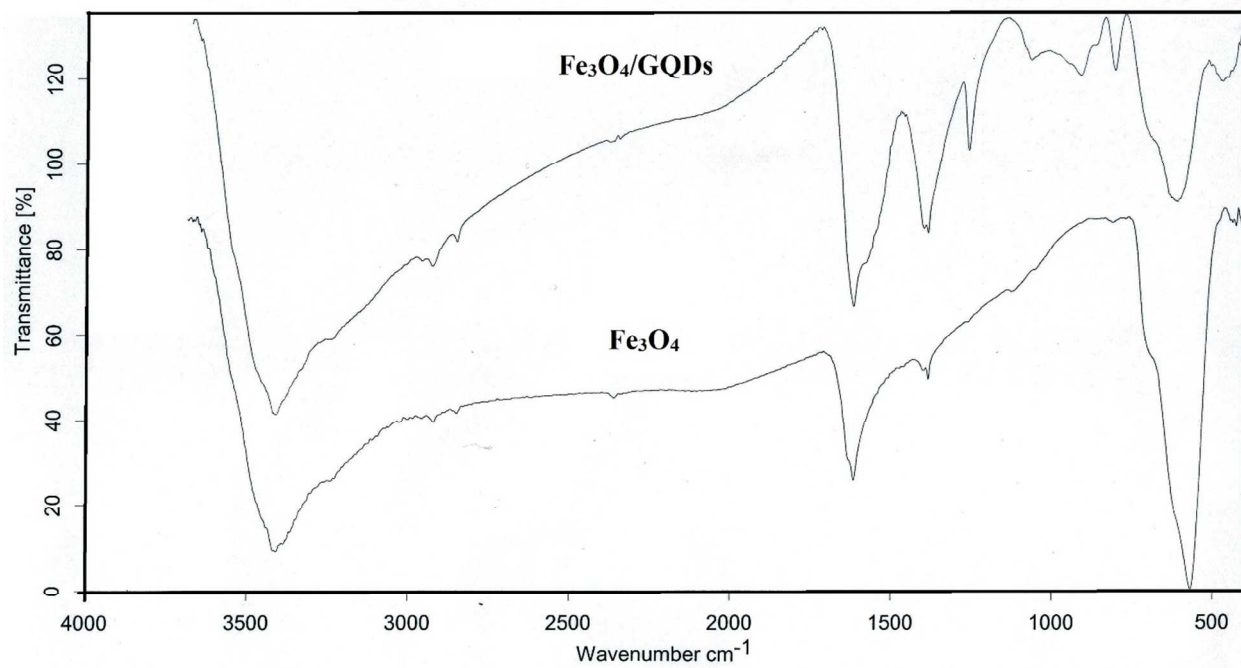


Fig. 1

1
2
3
4
5
6
7
8
9
10
11
12
13
14
15
16
17
18
19
20
21
22
23
24
25
26
27
28
29
30
31
32
33
34
35
36
37
38
39
40
41
42
43
44
45
46
47
48
49
50
51
52
53
54
55
56
57
58
59
60

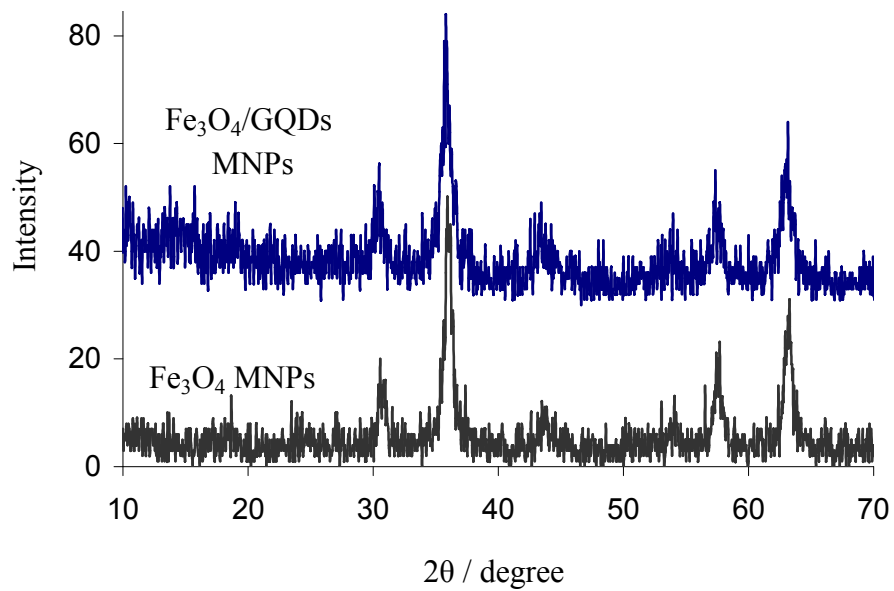


Fig. 2

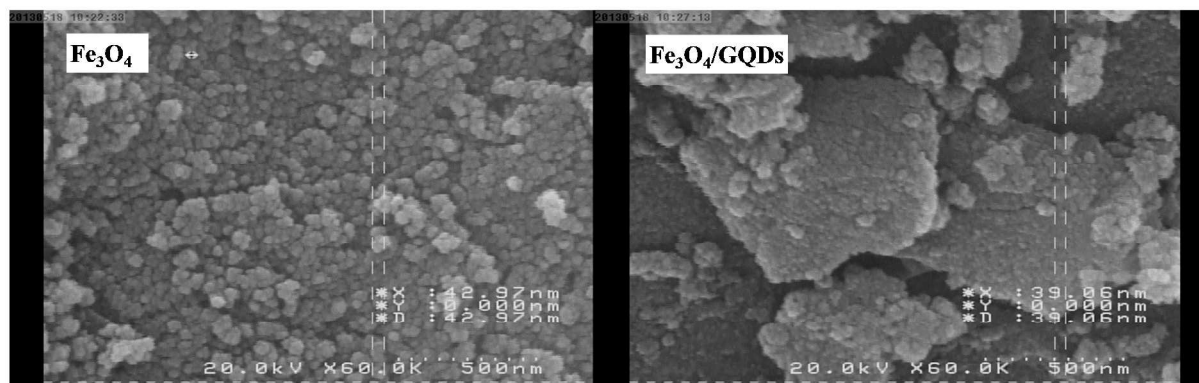


Fig. 3

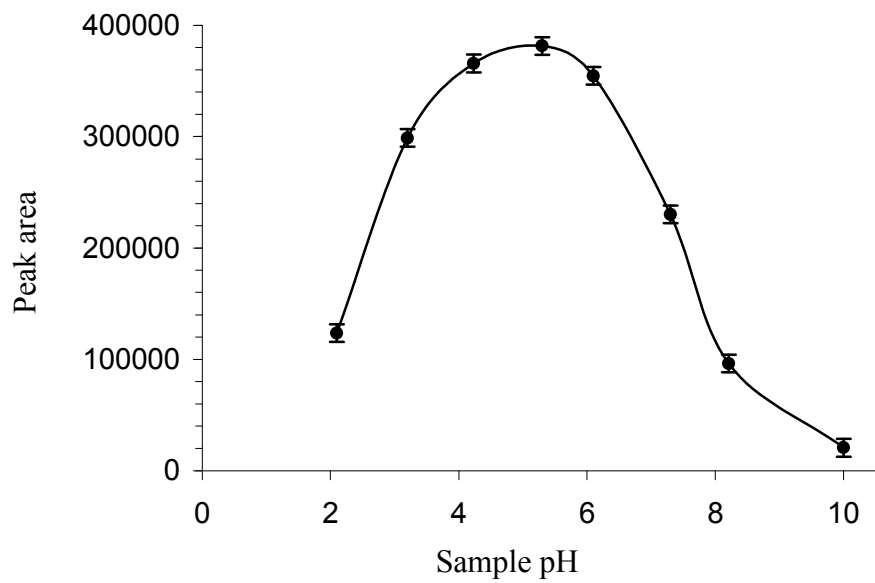


Fig. 4

1
2
3
4
5
6
7
8
9
10
11
12
13
14
15
16
17
18
19
20
21
22
23
24
25
26
27
28
29
30
31
32
33
34
35
36
37
38
39
40
41
42
43
44
45
46
47
48
49
50
51
52
53
54
55
56
57
58
59
60

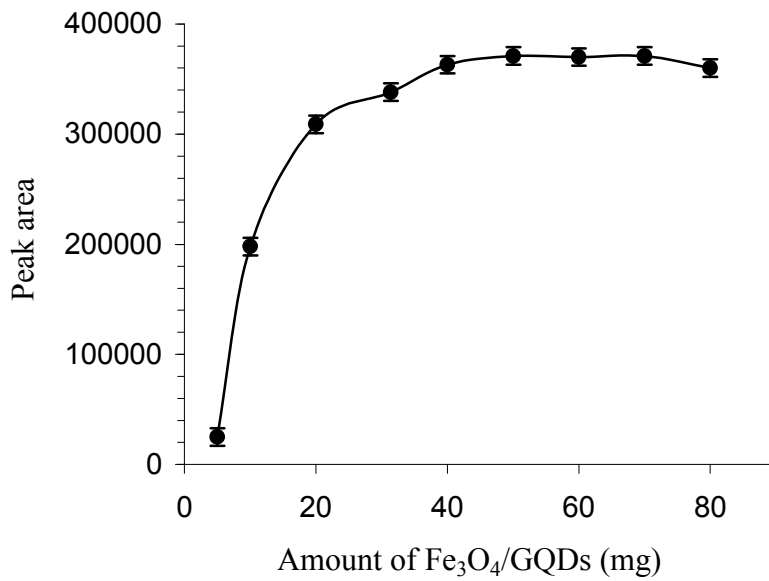


Fig. 5

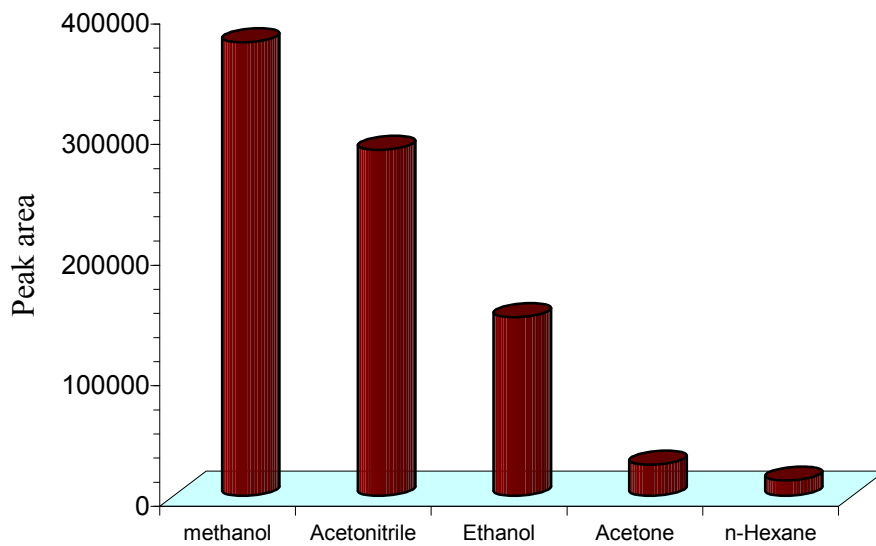


Fig. 6

1
2
3
4
5
6
7
8
9
10
11
12
13
14
15
16
17
18
19
20
21
22
23
24
25
26
27
28
29
30
31
32
33
34
35
36
37
38
39
40
41
42
43
44
45
46
47
48
49
50
51
52
53
54
55
56
57
58
59
60

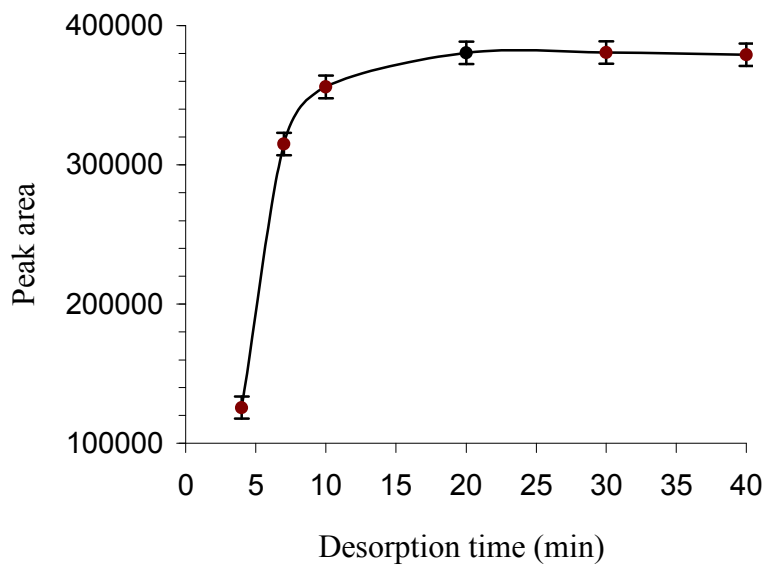


Fig. 7

1
2
3
4
5
6
7
8
9
10
11
12
13
14
15
16
17
18
19
20
21
22
23
24
25
26
27
28
29
30
31
32
33
34
35
36
37
38
39
40
41
42
43
44
45
46
47
48
49
50
51
52
53
54
55
56
57
58
59
60

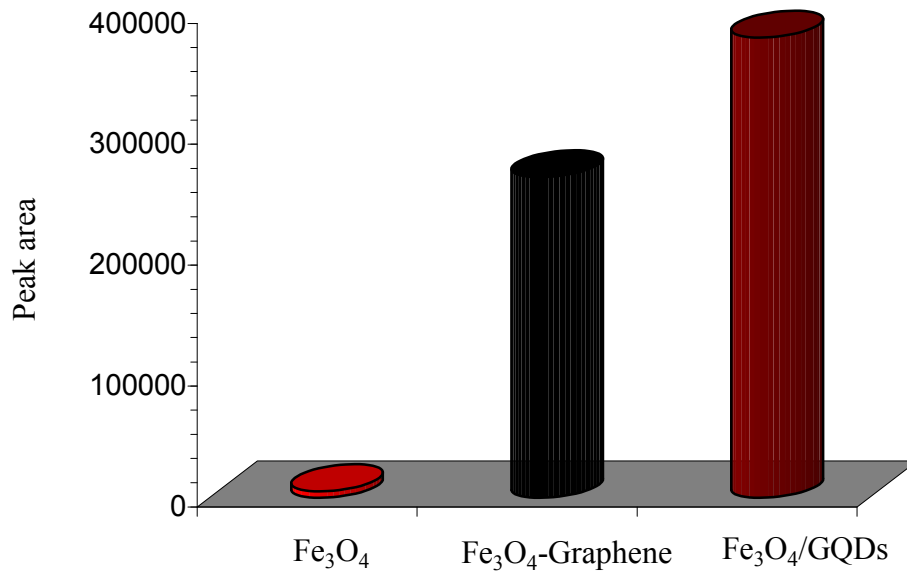


Fig. 8

1
2
3
4
5
6
7
8
9
10
11
12
13
14
15
16
17
18
19
20
21
22
23
24
25
26
27
28
29
30
31
32
33
34
35
36
37
38
39
40
41
42
43
44
45
46
47
48
49
50
51
52
53
54
55
56
57
58
59
60

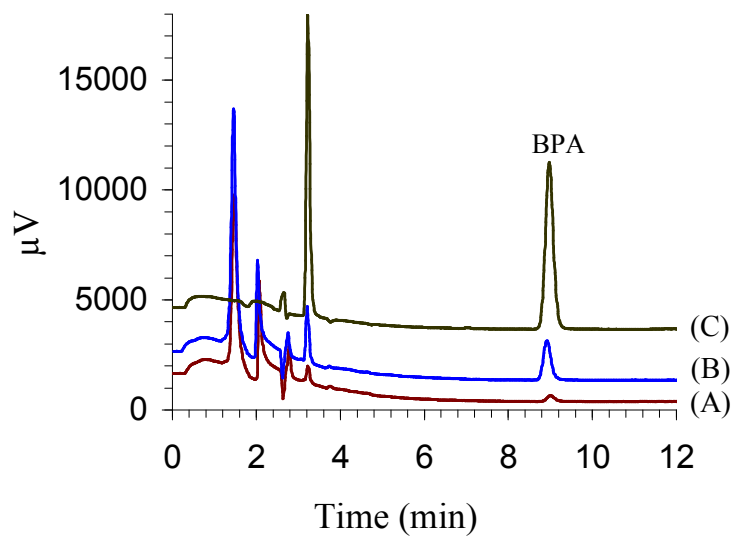


Fig. 9

Table. 1. Precision, LOQ, LOD, EF, Linearity, and regression equation obtained for BPA analysis

<i>Analyte</i>	<i>RSD (%)</i>	<i>LOQ (pg mL⁻¹)</i>	<i>LOD (pg mL⁻¹)</i>	<i>EF</i>	<i>LR (ng mL⁻¹)</i>	<i>Regression equation</i>
BPA	4.3	41	12.3	360	0.1-300	Y= 3606 X +20266

Table 2. Results of determination and recoveries of mineral water samples spiked with BPA

<i>Amounts of BPA (ng mL⁻¹)</i>	<i>R.S.D. (%)</i>	<i>Recovery (%)</i>
5	5.2	96.3
10	4.3	104.9
20	3.6	98.5

1
2
3
4
5
6
7
8
9
10
11
12
13
14
15
16
17
18
19
20
21
22
23
24
25
26
27
28
29
30
31
32
33
34
35
36
37
38
39
40
41
42
43
44
45
46
47
48
49
50
51
52
53
54
55
56
57
58
59
60